Microelectromechanical Organs-on-Chip

Mastrangeli, Massimo; Aydogmus, Hande ; Dostanic, Milica; Motreuil-Ragot, Paul ; Revyn, Nele; de Wagenaar, Bjorn; Dekker, Ronald; Sarro, Pasqualina M.

DOI
10.1109/Transducers50396.2021.9495646

Publication date
2021

Document Version
Final published version

Published in
21st International Conference on Solid-State Sensors, Actuators and Microsystems, TRANSDUCERS 2021

MICROELECTROMECHANICAL ORGANS-ON-CHIP

Massimo Mastrangeli, Hande Aydogmus, Milica Dostanic, Paul Motreuil-Ragot, Nele Revyn, Bjorn de Wagenaar, Ronald Dekker, and Pasqualina M. Sarro*
ECTM, Department of Microelectronics, Delft University of Technology, the Netherlands

2021 21st International Conference on Solid-State Sensors, Actuators and Microsystems (Transducers) | 978-1-6654-1267-4/21/$31.00 ©2021 IEEE | DOI: 10.1109/TRANSDUCERS50396.2021.9495646

ABSTRACT

Stemming from the convergence of tissue engineering and microfluidics, organ-on-chip (OoC) technology can reproduce *in vivo*-like dynamic microphysiological environments for tissues *in vitro*. The possibility afforded by OoC devices of realistic recapitulation of tissue and organ (patho)physiology may hold the key to bridge the current translational gap in drug development, and possibly foster personalized medicine. Here we underline the biotechnological convergence at the root of OoC technology, and outline research tracks under development in our group at TU Delft along two main directions: fabrication of innovative microelectromechanical OoC devices, integrating stimulation and sensing of tissue activity, and their embedding within advanced platforms for pre-clinical research. We conclude with remarks on the role of open technology platforms for the broader establishment of OoC technology in pre-clinical research and drug development.

KEYWORDS

Actuators, microelectrode arrays, microfabrication, organ-on-chip, open technology platforms, sensors, tissues

INTRODUCTION

Well into its second decade of development following its formal inception [1], organ-on-chip (OoC) currently stands as a thriving biotechnological field. OoC technology, posed at the confluence of tissue engineering and micromechanics (Fig. 1), is expected to gain further momentum as well as market relevance in the short-to-midterm [2]. Demonstrations of the capability of OoC devices to reproduce physiologically representative microenvironments for tissue cultures *in vitro* are steadily accumulating [3]. The demonstrations are also backed by evidence of phenotypic expressions in OoC-hosted tissues which match expectations from *in vivo* conditions and are instead not manifested by the same tissues otherwise [4].

The realistic (patho-)physiological recapitulation enabled by OoC devices springs from the synergy of several distinguishing features [2], including eminently the provision of dynamic multi-modal stimulation, and of fluidic perfusion in particular. Time-varying stimuli of mechanical (*e.g.*, strain [1], shear stress [5]), electrical (*e.g.*, pacing [6]), optical (*e.g.*, optogenetic [7]) and chemical nature [8] promote and sustain tissue maturation, whereas tuneable media perfusion, possibly associated with tissue vascularization, can significantly extend the viability of tissues [9]. OoC devices can additionally provide continuous monitoring of tissue conditions and of microenvironmental parameters, complementing and extending the scope of optical imaging and sensing by means of electrical, mechanical and chemical sensors [10, 11].

Notably, integrated stimulation and monitoring functions, standing as partly unmet needs for OoC devices [2], largely correspond to the typical actuation and sensing functionalities afforded by microelectromechanical systems (MEMS). The biotechnological convergence between MEMS and tissue engineering which lies at the foundation of OoC is further motivated by a suitable correspondence of scales. The typical size of the basic functional units (*i.e.*, organoids) composing most of human organs is commensurate to the typical dimensions or feature sizes of common MEM devices (*i.e.*, hundreds of microns) [12]. Besides by functional and size matching, microfabrication technologies suit OoC requirements by enabling the manufacturing of structures and systems spanning a wide spectrum of sophistication and complexity [13] – from fluidic polymeric modules fabricated by soft lithography [1, 5] to integrated multi-material high-throughput platforms [14]. Multiple solutions which conveniently fit the application or user-defined purpose of an OoC device can accordingly be conceived. On the one hand, the vast freedom in design and fabrication supported by such technologies has permitted the emergence of very diverse device concepts and imple-

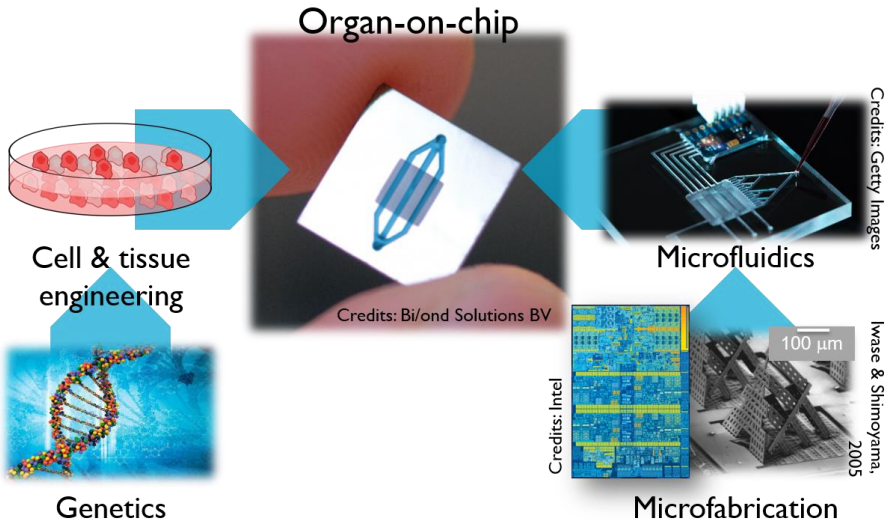

Figure 1. The biotechnological convergence at the root of OoC technology.

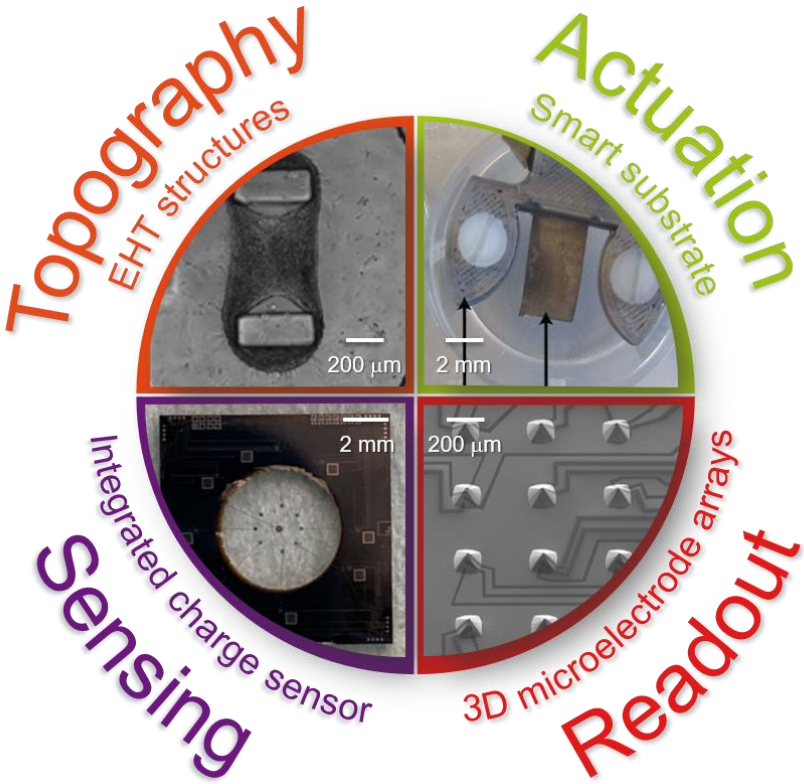

Figure 2. Examples of microelectromechanical silicon- and polymer-based OoC devices.
Top left: a 1 uL-derived (~16000 cells) engineered heart tissue self-assembled across a pair of elastic polymer micropillars [21].
Top right: an 8-mm long IPMC cantilever fitting in a single well of a 12-well plate by means of a custom electrode holder [30].
Bottom left: a silicon frame embedding 8 floating-gate field-effect transistors and supporting an optically transparent PDMS membrane. Extensions of the floating gates (sensing electrodes) and a central electrode reach across the suspended membrane [35].
Bottom right: array of anisotropically etched Si micropyramids, each featuring three vertically stacked and electrically independent TiN microelectrodes [25].

mentations. Such richness of solutions has allowed a significant number of the main human organs and tissues to be recapitulated by specific OoC models [2]; and it proves additionally beneficial, since it appears clear that a single type of OoC device is unlikely to meet all needs and fit all application purposes [3]. On the other hand, such device diversification, when not coordinated by concerted OoC validation [4] and standardization [15] approaches, may risk to fragment the OoC landscape into a constellation of hardly compatible point solutions which might not reach significant research or commercial fruition. The latter scenario would hinder the coherent development and wider acceptance of the technology [2-4].

In this paper we outline the ongoing research activity of our group at TU Delft in the development of innovative silicon- and polymer-based MEM OoC devices, and their perspective integration within open technology platforms (OTPs). We aim to exemplify as well how a consistent set of biocompatible materials and corresponding wafer-level processing techniques can be browsed and combined by a user to fabricate tailored OoC devices. Our activity is furthermore embedded in a more general collaborative context conducive to technology standardization and user accessibility [3]. The key role of OTPs for the further establishment of OoC technology in pre-clinical research and drug development is emphasized in the concluding remarks.

MEMS-FLAVORED OOC DEVICES

To best fit their purpose, OoC devices should be as simple as possible, and only as complex as needed. The complexity of OoC devices should only ensue from their purpose, and rather not compromise their ease of use [2]. Soft lithography [16] and injection moulding [17] are the fabrication techniques of choice respectively for fast prototyping of simple microfluidic chip modules and for large volume production of high-throughput titer plate-based devices. Together, they currently account for the production of the majority of OoC devices, as well as for their early adoption respectively in biological research and pre-clinical drug development. However, integration of actuators and sensors within such devices is challenging and compromises the scalability of the fabrication process. Wafer-scale silicon- and polymer-based microfabrication allows for highly-reproducible batch device fabrication. It thus represents an interesting alternative for OoC manufacturing – one which is amenable both to upscaling to high-volume production and to seamless integration of transductive functionalities within physiologically relevant microsystems [18].

As a partial showcase of the possibilities delivered by a seamless combination of silicon- and polymer-based microfabrication techniques into single process flows, in the following sections we briefly present the main directions of our material and device research for OoC (Fig. 2) according to the increasing complexity of the devices.

Topography: engineered heart tissue structures

Efficient development of effective drugs for cardiovascular diseases, the most common cause of death worldwide, has high societal priority. A proposed alternative to overcome the limitations of animal and *in vitro* cell culture models is engineered heart tissues (EHTs). These human cardiac tissue models were reported to recapitulate human heart responses more closely than 2D cell cultures [19], and are thus a promising tool for cardiac drug testing and disease modelling. EHTs are formed by the self-assembly of cardiac cells in the presence of extracellular matrix proteins into a beating cardiac muscle strand around flexible anchoring points. Different shapes and numbers of the anchoring points and sizes of the tissues were reported [20].

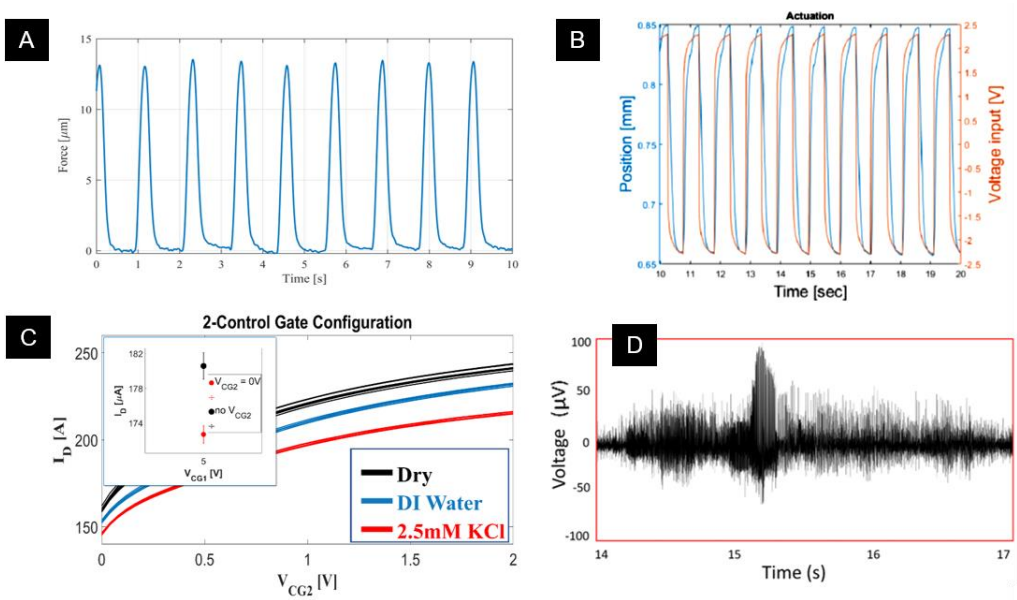

Figure 3. Sensing and actuation enabled by microelectromechanical OoC devices (refer to Fig. 2). A) Contraction force exerted by a 3 μL-derived engineered heart tissue, estimated by software-based optical tracking of micropillar displacement [21]. B) Displacement of an 8 mm-long IPMC cantilever driven by low input voltage (5 Vpp, 1 Hz) [30]. C) Analyte detection from the output characteristics of a dual-gate nMOS-based electrochemical charge sensor [35]. D) Single-channel trace of a 3D MEA recording with hiPSC-derived cortical neurons matured for 25 days on chip (courtesy of M. Hu and J.-P. Frimat, Leiden Medical University Center) [25].

We developed miniaturized EHT structures which require less than 50000 cells per data point and can be structurally characterized with great accuracy by mechanical nanoindentation (Fig. 2, top left) [21]. The basic EHT structure, made of polydimethylsiloxane (PDMS), is composed of a pair of vertical micropillars surrounded by an elliptical microwell of similar height, and represents an anisometrically downscaled version of the Heart-Dyno system [22]. The downscaling allowed to reduce the number of cells required per EHT and to make the fabrication compatible with batch wafer-level processing, while retaining the original pillar stiffness. The EHT structures were fabricated by casting PDMS over moulds made of hydrophobic, photolithographically patterned and deep reactive ion-etched silicon wafers. Upon demoulding, the EHT structures were transferred to the bottom of the wells in 96-well plates for self-assembly and testing of the EHTs. Mixtures of human-induced pluripotent stem cell (hiPSC)-derived cardiomyocytes and hiPSC-derived cardiac fibroblasts were seeded in EHT structures of volume varying from 3 μL (47000 cells) down to 1 μL (16000 cells). All tissues formed successfully and were functionally active. Contractile properties of the tissues, including beating dynamics and contraction force, were evaluated by optically tracking the movement of the PDMS micropillars (Fig. 3A). The tissues were viable and functional for at least 18 days. In experiments with external electric stimulation, the miniaturized EHTs followed the pacing frequency up to 2.4 Hz.

By showing that elastomeric topographical microstructures could be conveniently realized using scalable fabrication methods, we came closer to high-throughput cardiac drug screening and disease modelling using OoC technology. Moreover, silicon- and polymer-based microfabrication opens many opportunities for further upgrades of the EHT devices, including integration of pacing electrodes and of electric sensors for automated signal readout.

Readout: segmented 3D microelectrode arrays

Reproducing full neuronal functionality realistically on a chip requires cell cultures that exhibit intercellular interactions in three dimensions (3D) [23]. Tracking *in vitro* the full extent of 3D interactions in a neuronal tissue would significantly advance the study of dynamic neural network activity, prompting in particular the analysis of collective patterns of neuron activation which are associated with delocalized pathologies such as *e.g.* migraines and cortical spreading depolarization. Achieving this requires electrophysiological sampling distributed along all three spatial dimensions, which standard 2D microelectrode arrays (MEAs) cannot perform [24]. To address this need, we fabricated novel 3D MEAs composed of 2D arrays of Si micropyramids, each micropyramid being endowed with multiple, electrically distinct and vertically stacked microelectrodes (Fig. 2, bottom right) [25]. The unique design and implementation of the microelectrodes allows for 3D single-unit recordings with high throughput, which is currently not possible on commercial MEAs [26].

The fabrication of the 3D MEAs entailed timed anisotropic wet etching (25% TMAH + Triton) through a patterned SiN hard mask oriented with respect to the crystal planes of a 4'' Si wafer [27]. This yielded 5-by-4 arrays of ~90 μm-high truncated Si micropyramids with ~20 μm-wide plateau and lateral facet slope ranging from ~46° to ~53°. The micropyramids were electrically passivated with thermally-grown SiO_2, and a 10nm/150nm-thick Ti/TiN layer was then sputtered and lithographically patterned to define three electrically independent microelectrodes over the slanted facets of each pyramid, totaling 60 electrodes per array. A second SiO_2 layer was later deposited and etched away at predefined locations to finalize the vertically stacked sampling points on each pyramid. 18-by-18 mm^2 chips were diced out of the wafer and wire-bonded to

square printed circuit boards (PCBs) with 60 peripheral contact pads, making them compatible with the commercially available MEA2100 readout from Multichannel Systems [28]. The electrode background noise, measured with the MEA2100 readout system, was in the order of 20 μV.

Cortical neurons derived from hiPSCs were differentiated and matured on the 3D MEAs, and the cell cultures were monitored up until 25 days *in vitro* (DIV). The measurements of the hiPSC-derived cortical neurons (DIV25) showed clear network bursting activity as recorded through the 3D MEAs (Fig. 3D). The encouraging preliminary results prompt further analyses to record full electrical neuronal network activity in 3D. Future experiments are envisaged with brain organoids and 3D cell constructs over optically transparent variants of our 3D MEAs.

Actuation: electro-active polymer-based substrate

Growth and maturation of tissues such as *e.g.* alveolar [1], intestinal [5], cardiac [19] and cardiovascular [29] require forms of mechanical stimuli. To date, substrates for cell cultures in OoC devices have been mainly actuated pneumatically by means of external systems. The latter are typically bulky, expensive and nonuser-friendly, and may thus limit the adoption of OoC devices by researchers and industry. To overcome this limitation, we proposed the first actuating and sensing smart material-based OoC device (Fig 2, top right), and demonstrated its functionality by culturing human vascular smooth muscle cells (vSMC) [30].

Our device utilizes a single ionic polymer metal composite (IPMC)-based transducer to provide both actuation and sensing to cell cultures. The IPMC substrate was manufactured by electroless deposition of Pt on a commercial, 180 mm-thick Nafion-117 membrane using iterative immersion-reduction steps [31]. The soft IPMC substrate allows to intermittently apply cyclic loading to tissues and to sense their spontaneous contractions. In actuation mode, a voltage difference applied across the electrode pair induces migration of the loosely coupled cations within the membrane, causing the cantilever-shaped IPMC to bend and thus to strain the cells cultivated on the IPMC surface. In sensing mode, the intrinsic contraction of the cells induce a deformation of the IPMC and consequent displacement of the cations, leading to a voltage drop across the electrodes which can be measured as a readout signal.

We integrated the IPMC-based transducer within a compact and easy-to-operate OoC device, fitting a 12-well plate and connected to a custom electronic board driving actuation and signal readout. The 8 mm-long IPMC prototype achieved an actuation range of 0.2 mm (Fig. 3B) and 0.72 V/mm sensing resolution. The 0.1 % strain correspondingly induced by actuation on the cells accurately corresponds to *in vivo* strain values for vSMCs. We successfully grew vSMCs on the IPMC substrate, and actuated them for 150 min at 1 Hz. Fluorescent staining showed no evidence of adverse effects. These results are a promising step towards the fabrication of versatile, all-electric OoC devices for a variety of biological models of human tissues.

Sensing: integrated FET-based charge sensor

To reduce user intervention, improve ease of use and enhance reliability of OoC devices, continuous automated monitoring of biological cues is highly demanded [2]. Many metabolic cues consist of charged species, and they can be quantitatively detected by biochemical and electrochemical sensors [32] without recurring to microscopy techniques and terminal optical labelling, which considerably perturb the physiology of cells.

In this regard, we have demonstrated the integration of electrochemical charge microsensors within a MEM OoC device [33]. The 1-by-1 cm^2 OoC device is composed by a rigid silicon frame supporting a soft and optically transparent polymer membrane, and is fabricated by a largely CMOS-compatible process flow (Fig. 2, bottom left). Such hybrid OoC device combines in a single chip the benefit of a soft substrate, suitable for culturing tissues under mechanobiologically relevant conditions, with that of extremely compact and inherently signal-amplifying electronic sensing units, uniquely enabled by silicon-based microfabrication [34]. The sensors are based on floating-gate field-effect transistors (FG-FETs), whose Ti floating gate electrode extends across the suspended PDMS membrane representing the tissue culturing area. Charges in proximity of the sensing electrode induce a polarization of the electrode, which in turn shifts the threshold voltage of the FET. Charges in the culture area can therefore be continuously detected by monitoring the transistor's drain current.

We have additionally shown significant enhancement in sensitivity and in selective response of the FG-FET-based charge sensor by the introduction of a novel dual-control-gate configuration and of *in situ* decoration of the sensing electrode surface with nanoporous Au thin films [35]. This enhanced sensor replaces the function of an external reference electrode with that of a pair of control gates capacitively coupled to the floating gate. Bias on one of the control gates provides electric field towards the extension of the floating gate on the culturing area. This promotes the binding of charged species on the sensing surface of the electrode, and thus higher sensitivity. In addition, we deposited microscopically rough Au films on the sensing electrode surface by inertial impaction at room temperature of pure Au nanoparticle aerosol generated by spark ablation. This *in situ* post-fabrication surface structuring step increased the effective sensing area, and more than doubled the sensitivity as a result. The technique is maskless, spatially-selective, fast, and does not harm the polymer membrane supporting the sensing electrodes.

The OoC-integrated charge sensor could be used to successfully identify different solutions, including low-concentration poly-D-lysine and KCl (Fig. 3C). Furthermore, neural progenitor cells were successfully differentiated to cortical neurons on our OoC device, attesting its biocompatibility. These preliminary results suggest that our MEM OoC device may be employed to quantify the level of potassium ions (K^+) of human brain cells, a crucial indicator for the wellbeing and functioning of the brain [36].

FROM OOC DEVICES TO PLATFORMS

The establishment of open technology platforms (OTPs) is considered as a most congenial route to address at once and at system level the need for standardization, ease of use, and compatibility with existing laboratory infrastructure and workflows of OoC devices [3]. A comprehensive OTP should ideally include aspects of both hardware (*e.g.*, footprint, materials, functionalities, interfaces) and software

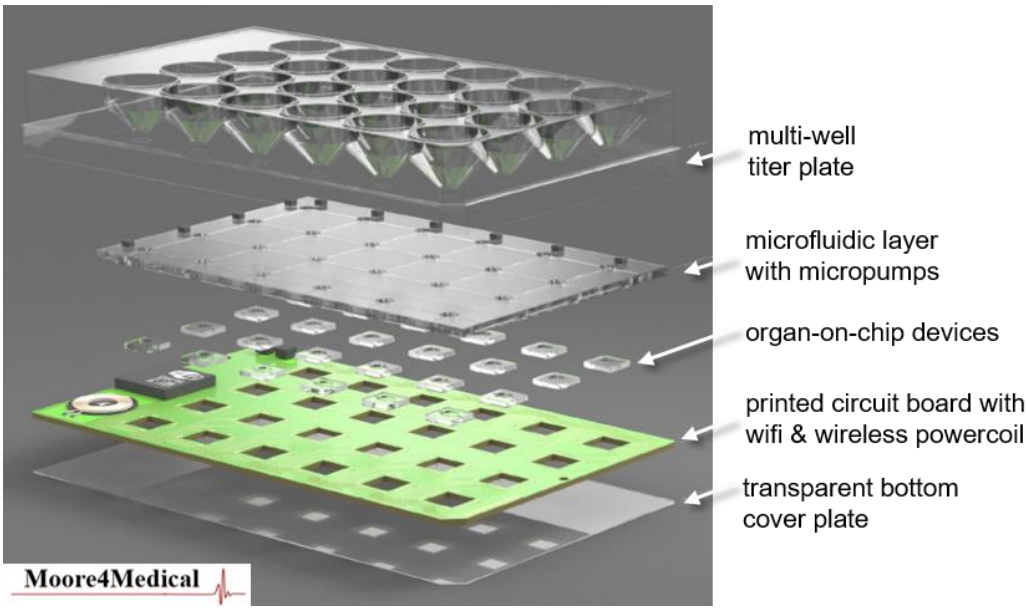

Figure 4. Main components of Moore4Medical's smart multi-well plate OoC platform [39]. (An animated illustration of the SMWP concept and architecture is available at the following address: https://youtu.be/H595oGbMdyM).

(*e.g.*, data analysis software, data formatting), and provide end users with the possibility to compose their OoC device out of the available set of technological options to best fit their purpose. Motivated by the strategic advantages and commercial success that OTPs have contributed to introduce in the domain of electronic components and systems (ECS), the deployment of OTPs for OoC is similarly expected to lower the penetration barrier and prompt broader adoption of the technology. Current examples of OoC platforms include the Translational OoC platform (TOP) developed at University of Twente [37], the high-throughput OoC platform from Draper [14], and the Cytostretch, a MEM OoC platform developed in our lab [18, 38].

The OoC research tracks described in the previous sections are themselves being pursued as OTPs, whereby material selection and process flows could be transferred to MEMS foundries for eventual upscaling and larger commercial fruition. In addition, we aim to make our OoC devices compatible with the aforementioned TOP and with the smart multi-well plate (SMWP) platform, currently under development in the Moore4Medical ECSEL-JU project [39]. The SMWP is conceived as a standardized and standalone multi-well plate for the full automation of OoC assays and workflows. As shown in Fig. 4, the SMWP is composed of four main functional layers: an open-top titer plate with standard footprint (ANSI/SBS); an OoC layer, configurable with OoC devices with standardized footprint and electric and fluidic interfaces, and produced by different providers; a microfluidic distribution layer embedding the OoC devices within microfluidic circuits driven by integrated piezoelectric micropumps; and an electric distribution layer in the form of a suitable PCB, driving on-chip sensors and electrode readout, and hosting a wireless power transfer and a wireless data transfer module. The layers are packaged within a plastic encasing with optically transparent bottom cover plate, providing hermetic sealing for use of the SMWP in standard incubator environments for cell cultures and advanced OoC biological assays. Accordingly, the SMWP is expected to fit seamlessly into existing laboratory infrastructure and automated workflows based on multi-well plates, so to extend their monitoring, stimulation and data collection functionalities through OoC-integrated microfluidics, transducers, and data transfer.

CONCLUSION

MEMS technology provides many relevant opportunities for advancing and scaling up OoC technology. Though examples from our ongoing MEM OoC research tracks, we have showcased how MEMS technology can enable integrated actuation and sensing functionalities to respectively stimulate and monitor the activity of cell constructs within physiologically realistic microenvironments, as well as introduce ample variety in multi-material structuring and functionalization. Embedding OoC devices into OoC platforms based on open technology and shared design standards is expected to further increase OoC adoption by researchers and industrial end users, and ensure the smooth establishment of OoC technology into existing laboratory practice, workflows, and infrastructure. Together with current concerted efforts in qualification and testing of the devices [3, 4], this should bring OoC technology closer to fulfilling its potential towards more effective drug development, personalized medicine, and advancing knowledge of human physiology.

ACKNOWLEDGEMENTS

The authors thank the staff at the Else Kooi Laboratory of TU Delft for their support with microfabrication, all our colleagues at the Leiden University Medical Center for cultivating cardiac and neuronal tissues on our devices, and the WP2 partners of the Moore4Medical consortium.

This work was supported by the Netherlands Organ-on-Chip Initiative, an NWO gravitation project funded by the Ministry of Education, Culture and Science of the government of the Netherlands (024.003.001), and by the "Moore4Medical" project funded by the ECSEL Joint Undertaking under grant agreement H2020-ECSEL-2019-IA-876190.

REFERENCES

[1] D. Hu *et al.*, *Science* 328, pp. 1662-1668, 2010.
[2] M. Mastrangeli *et al.*, *ALTEX* 36(4), p. 650-668, 2019.
[3] M. Mastrangeli *et al.*, *ALTEX* 36(3), p. 481-492, 2019.
[4] U. Marx *et al., ALTEX* 37(3), pp. 365-394, 2020.
[5] H. J. Kim *et al., Lab Chip* 12, pp. 2165-2174, 2012.
[6] A. Marsano et al., Lab Chip 16, pp. 599-610, 2016.
[7] T. Osaki *et al., Sci. Adv.* 4(10), eaat5847, 2018.
[8] P. E. Oomen *et al., Lab Chip* 16, p. 3394-3414, 2016.
[9] I. Maschmeyer *et al., Lab Chip* 15, p.2688-2699, 2015.
[10] J. Wikswo *et al., IEEE Trans. Biomed. Eng.* 60(3), pp. 682-690, 2013.
[11] J. Kieninger *et al., Lab Chip* 18, pp. 1274-1291, 2018.
[12] U. Marx *et al., ATLA* 40(5), pp. 235-257, 2012.
[13] B. Zhang *et al., Nat. Rev. Mater*. 3, pp. 257-278, 2018.
[14] H. Azizgolshani *et al., Lab Chip* 21, 1454-1474, 2021.
[15] D. R. Reyes *et al., Lab Chip* 21, pp. 9-21, 2021.
[16] D. B. Weibel *et al., Nat. Rev. Microbiol.* 5, pp. 209-218, 2007.
[17] M. Heckele & W. K. Schomburg, *J. Micromech. Microeng.* 14, pp. R1-R41, 2003.
[18] N. Gaio *et al., Micromachines* 7(7), 120 (14pp), 2016.
[19] J. M. Stein *et al., Stem Cell Rep.,* DOI: 10.1016/j.stemcr.2020.11.013, 2020.
[20] I. Jorba *et al., Tissue Eng. C*, 27(3), pp. 139-151, 2021.
[21] M. Dostanic *et al., JMEMS* 29(5), pp. 881-887, 2020.
[22] R. J. Mills *et al.*, *Proc. Natl. Acad. Sci* 114 (40), pp. E8372-E8381, 2017.
[23] J. L. Bourke *et al.*, *J. Tissue Eng. Regen. Med.* 12, pp. 490-493, 2018.
[24] C. M. Didier *et al.*, *J. Micromech. Microeng.* 30, 103001 (28pp), 2020.
[25] N. Revyn *et al., EUROoCS 2021*.
[26] J. S. Choi *et al., Biosens. Bioelectr.* 171, 112687, 2021.
[27] M. M. Smiljanic et al., Micromachines 10(2), pp. 102-115, 2019.
[28] K. Musick et al., *Lab Chip* 9, pp. 2036-2042, 2009.
[29] W. Zheng *et al., Lab Chip* 12, pp. 3441-3450, 2021.
[30] P. Motreuil-Ragot *et al., RoboSoft 2020,* pp. 530-533.
[31] M. Shahinpoor *et al., Smart Mat. Struct*. 7, pp. R15-R30, 1998.
[32] M. Oliveira *et al.*, *Cancers* 13, 1381 (21 p)., 2021
[33] H. Aydogmus *et al., IEEE SENSORS 2020*. pp. 1-4.
[34] M. Kaisti., *Biosens. Bioelectron*. 98, 437-448, 2017.
[35] H. Aydogmus *et al., TRANSDUCERS 2021*.
[36] C. Simons *et. al*., *Nat. Genetics*, pp. 47, 73–77, 2015.
[37] A. R. Vollertsen *et al., Microsyst. Nanoeng.* 6, 107 (16pp), 2020.
[38] N. Gaio *et al., IEEE MEMS 2018*, pp. 314-317.
[39] "Moore4Medical" ECSEL-JU project, available at: https://moore4medical.eu/.

CONTACT

*M. Mastrangeli, m.mastrangeli@tudelft.nl